

# Wave energy farm design in real wave climates: the Italian offshore

Silvia Bozzi <sup>1\*</sup>, Marianna Giassi <sup>2</sup>, Adrià Moreno Miquel <sup>3</sup>, Alessandro Antonini <sup>4</sup>, Federica Bizzozero <sup>1</sup>, Giambattista Gruosso <sup>1</sup>, Renata Archetti <sup>3</sup> and Giuseppe Passoni <sup>1</sup>

<sup>1</sup> Department of Electronics, Information Science and Bioengineering, Politecnico di Milano, Piazza Leonardo da Vinci 32, 20133 Milano, Italy

<sup>2</sup> Department of Engineering Sciences, The Ångström Laboratory, Uppsala University, Box 534, 75121 Uppsala, Sweden

<sup>3</sup> Department of Civil, Environmental and Materials Engineering, Università di Bologna, Viale Risorgimento 2, 40136 Bologna, Italy

<sup>4</sup> Coastal, Ocean and Sediment Transport Research Group - Plymouth University - Marine Building, Drake Circus, Plymouth, Devon, PL48AA, UK

\* Author to whom correspondence should be addressed; E-Mail: [silvia.bozzi@polimi.it](mailto:silvia.bozzi@polimi.it); Tel.: +39-02-2399-4146; Fax: +39-02-2399-3360.

## Abstract:

The work focuses on hydrodynamic interactions between heaving wave energy converters (WEC). Wave parks of four devices are simulated in the time domain by a hydrodynamic-electromagnetic model, coupled with a boundary element code for the estimation of hydrodynamic parameters. Different layouts (linear, square and rhombus), WEC separation distances (5, 10, 20 and 30 buoy diameters) and incident wave directions (30° apart) are considered to assess the effect of design parameters on array power production. Then, a site-specific design optimization is carried out for different Italian locations and some key insights on wave farm design in real wave climates are provided. The results show that the effect of wave interactions on energy absorption is not expected to be a main issue, as long as the devices are separated by at least 10 buoy diameters and that the layouts are oriented to achieve the maximum energy absorption for the prevailing wave direction.

**Keywords:** renewable energy; wave energy; arrays; hydrodynamic interactions; numerical modelling; Italy.

## 1. Introduction

Since the renewed interest in wave energy conversion, following the 1973 oil crisis, significant advances have been made in modelling, design and optimization of wave energy converters. Wave to wire models coupled with boundary element methods (BEMs) for estimation of hydrodynamic parameters are now the state of the art and are currently used by WEC developers to assess device

performance, investigate control strategies and optimize geometry details [1]. Numerical tools have also been developed to simulate multiple interacting devices, as most of the wave energy converters are designed to be deployed in arrays of many units. A comparative analysis of the different modelling techniques can be found in Folley et al. [2]. However, simulating wave energy farms requires significant computational resources because it involves the solution of the scatter and radiation problem of all the units, for all the frequencies of interest. Moreover, the performance of WEC arrays depends on several design parameters, such as the number of devices, the distance between them, the direction of incident waves and the spatial layout. As such, parametric studies of wave energy farms are generally limited either in model accuracy or in the exploration of the parameter space (mainly the number of park units).

Most of the studies on WEC arrays have focused on small wave farms (2 – 10 devices) using semi-analytical representations of a potential flow solution, such as the point absorber approximation, the plane wave method or the direct matrix method [3-7]. More recently, BEM-based numerical codes have been used to get the full solution of the diffraction and radiation problems without limitations on buoy shape, geometrical layout and WEC distance [8-12]. It is argued that they are the only methods able to accurately predict hydrodynamic interactions in wave energy parks, but they are limited to small arrays, due to their high computational costs [13]. At present, large wave farms (more than 10-20 devices) can be only simulated by approximate methods based on one or more simplifying assumptions (e.g. [14,15]).

Pioneering works on array interactions (e.g. [3, 16]) studied simple wave farm configurations, namely optimally controlled axisymmetric buoys in unidirectional regular waves, to assess the effect of wave interactions on energy absorption. Successive studies analyzed more in detail the influence of different design parameters on wave farm performance. In the following, a short review of some selected works is reported. Babarit [9] assessed the influence of the distance between two wave energy converters on energy production. Child and Venugopal [17] focused on the arrangement of the devices within the array using both a genetic algorithm and a parabolic intersection method to identify the optimum park geometry for different combinations of wave number and direction. Borgarino et al. [10] presented a parametric study on arrays of nine to twenty-five generic WECs (heaving cylinders and surging barges) to assess the influence of interactions between bodies on yearly energy production. De Andrés et al. [11] investigated the effect of different parameters (number of devices, geometry layout, WEC distance and wave direction) in arrays of three to five dual body heaving WECs. They also performed an analysis to assess the optimum array configurations, in terms of power production, for different wave climates around the globe. Michele et al. [18] analyzed the resonant behavior of a flap gate farm, highlighting the effect of gate thickness on system response to incident waves. Engström et al. [19] and Göteman et al. [12] studied array performance in terms of power fluctuations with the aim of identifying the array configurations with the lowest power variance. The former investigated the effect of array geometry on power fluctuations, while the latter considered also other design parameters, such as number of WECs, distance of separation among them and wave direction. Bacelli and Ringwood [20] and Garcia-Rosa et al. [21] studied the effect of different power take-off (PTO) control strategies on arrays of two and four heaving cylinders, respectively. Nambiar et al. [22] addressed the same issue for a three-float Wavestar device. Sharkey et al. [23] explored different strategies to reduce the cost of the electrical network, with a particular emphasis on submarine cables.

Despite the extensive literature on WEC arrays, the effect of wave directionality on array power production is poorly documented, even though wave direction is believed to be a key parameter to choose the best orientation of wave energy farms and achieve a maximum in production. In particular, studies on wave farm optimization in real – multidirectional - wave climates are still lacking. Existing works have addressed the issue assuming unidirectional seas, i.e. assessing the influence of different wave attack angles on array performance, without summing the effects over different wave directions. These studies have showed that an array configuration, which is optimal for a given wave incident direction performs poorly in some other directions. It was also demonstrated that the q-factor - the ratio between the power output of an array on  $N$  units and the power output of  $N$  isolated units – integrated over all incident wave directions must equals one, for a point absorber WEC [24]. Hence, if constructive interactions (q-factor  $> 1$ ) are achieved under a given wave attack angle, destructive interactions (q-factor  $< 1$ ) must dominate in some other directions. This result has led to the currently prevailing view that destructive interactions would prevail in real wave climates, unless they are characterized by small variations (less than  $30^\circ$  according to Thomas [25]) in wave directionality [13]. However, this conclusion has not been yet confirmed by wave farm studies in real – multidirectional - wave climates. As a result, it is still an open question if it is possible to design a wave energy farm in order to achieve some gain in the power output, due to constructive wave interference, or if positive wave interaction effects are only possible for specific combinations of wave period, wave direction, array layout and WEC separation distance, which are not realizable in real cases.

In this work, this issue is addressed by simulating a wave farm composed of four heaving point absorbers by a fully coupled wave-to-wire time domain model, which allows to account for the effect of array interactions on the power take off system. Arrays design parameters (geometrical layout, separating distance among the units, wave direction) have been changed in order to estimate the energy production of different wave farm configurations at four sites off the Italian coasts: Alghero, Mazara del Vallo, Ponza and La Spezia. The work aims at (i) assessing the effect of wave interactions on array power absorption in real wave climates and (ii) identifying the optimal designs of a 4 WECs array to be deployed off some selected locations along the Italian coasts. Ultimately, the work attempts to answer to the following key questions: is it possible to find array configurations (i.e. combinations of layout geometry, WEC distance, and orientation) that perform better than four isolated devices in real wave climates (i.e. taking into account multiple wave directions)? Which are the array geometries with the highest energy production in unidirectional, bidirectional and multidirectional wave climates? Does WEC separation distance influence the selection of the optimum layout? Which are the array configurations more suitable for the Italian wave climate?

The paper is organized as follows: the mathematical model of the wave farm is described in the next section. Simulation details are provided in section III. In section IV, the results for unidirectional waves are presented and discussed, showing the sensitivity of array performance to design parameters. Section V reports model application to real wave climates and presents the results for four Italian locations. Finally, in the last section, some conclusions are drawn.

## 2. Numerical model

The numerical model simulates the dynamics of an array of point absorbers oscillating in heave mode. More specifically, each device consists in a cylindrical buoy attached to a linear electric generator placed on the seafloor, similar to the WEC developed by Uppsala University Seabased WEC (e.g. [26-29]). This technology was selected as reference because it is one of the few which has undergone full-scale testing in real sea conditions and which is specifically designed for mild wave climates. However, the wave farm model can also be used to simulate other devices, as long as they are point absorbers with motion restricted to the heave mode.

The numerical model is based on linear potential flow theory, which relies on the following assumptions: inviscid and incompressible fluid, irrotational flow, small wave steepness, small wave height with respect to water depth and small body motions. The wave energy converters are modeled as single body systems (i.e. modelling the tether connecting buoy and translator as a rigid bar) with one degree of freedom along the vertical axis (heave mode), as this accounts for most of the movement [30]. All the devices in the array are assumed to have the same geometry and power take off characteristics. At this stage, forces due to the slack mooring system and to viscous drag are neglected. The time domain formulation of the model is based on the integro-differential equations first proposed by Cumming for ship motion [31] and later extended to oscillating-body WECs by Jefferys [32]. According to this approach, the equation of motion of  $N$  wave energy converters is cast in matrix form as:

$$(\mathbf{M} + \boldsymbol{\mu}_\infty)\ddot{\mathbf{z}}(t) = \mathbf{F}_{ex}(t) - \int_0^t \mathbf{K}_R(t - \tau)\dot{\mathbf{z}}(\tau)d\tau - (\mathbf{K}_H + \mathbf{K})\mathbf{z}(t) - \mathbf{F}_{PTO}(t) \quad (1)$$

where  $\mathbf{z}(t) = (\mathbf{z}_1(t), \mathbf{z}_2(t), \dots, \mathbf{z}_N(t))$  is the position vector of the array at time  $t$ , measuring deviations from the static equilibrium of each buoy;  $\dot{\mathbf{z}}(t)$  and  $\ddot{\mathbf{z}}(t)$  are the velocity and acceleration vectors of the array, respectively;  $\mathbf{M} = m\mathbf{I}$  is the mass matrix of the system, where  $m$  is the total mass of the device (buoy and translator) and  $\mathbf{I}$  is the identity matrix;  $\boldsymbol{\mu}_\infty$  is the infinite mass matrix;  $\mathbf{K}_H = k_H\mathbf{I}$  is the hydrostatic stiffness matrix, where  $k_H$  is the stiffness coefficient of the buoy, which accounts for the effect of gravity and buoyancy;  $\mathbf{K} = k\mathbf{I}$  is the spring stiffness matrix, where  $k$  is the elastic constant of the retracting spring attached to the translator, which allows to call it back during the wave trough phase; the time integral represents radiation forces, which are computed as a convolution of the body velocity with the radiation impulse response function  $\mathbf{K}_R(t)$ . The convolution integral accounts for the memory effect in the radiation force, which is due to the fact that waves radiated by the body at a given time theoretically affect the flow at all subsequent times. Practically, the kernel of the convolution integral decays rapidly and becomes negligible after a few tens of seconds [33]. Therefore, the infinite integration path was replaced by a finite time interval equal to the minimum value between  $15T_p$  and 75 s. The radiation impulse response function  $\mathbf{K}_R(t)$ , i.e. the radiation force exerted by the fluid after an impulsive velocity of the buoy at  $t = 0$ , was obtained from the corresponding frequency-domain data as follows:

$$\mathbf{K}_R(t) = \frac{2}{\pi} \int_0^\infty \mathbf{R}(\omega) \cos(\omega t) d\omega \quad (2)$$

where  $\mathbf{R}(\omega)$  is the radiation damping matrix of the array. This matrix is symmetrical, with the non-diagonal terms representing the mutual radiation forces among the different bodies.

$\mathbf{F}_{ex}(t)$  is the excitation force vector, due to incident and diffracted waves. As solution of the scattering problem where buoys are fixed in the waves, it can be calculated a priori. According to linear airy theory, real irregular waves can be represented as a superposition of  $N_w$  regular waves of amplitude  $A_i$ , frequency  $\omega_i$  and phase  $\varphi_i$ . Hence, the resulting excitation force was obtained as a superposition of the frequency components as follows:

$$\mathbf{F}_{exc}(t) = \sum_{i=1}^{N_w} \mathbf{F}_e(\omega_i) A_i \sin(\omega_i t + \varphi_i) \quad (3)$$

where  $\mathbf{F}_e(\omega)$  is wave excitation force in the frequency domain and the amplitude of the  $i$ -th wave component is given by:

$$A_i = \sqrt{2S(\omega_i)\Delta\omega} \quad (4)$$

where  $S(\omega_i)$  is the wave spectrum and  $\Delta\omega$  the frequency step. In the current study, the unidirectional JONSWAP spectrum  $S(H_S, T_p, \gamma)$  was adopted with a peak enhancement factor  $\gamma$  equal to 3.3 for all sea states [34]. The spectrum was discretized into a number of spectrum components equal to  $3T_{sim}/T_p$ , where  $T_{sim}$  indicates the length of the wave record derived by the spectral distribution. The frequency step of discretization was set equal to  $3/T_p$  and the  $i$ -th wave frequency was calculated as  $\omega_i = \omega_0 + i\Delta\omega$  with  $\omega_0 = 1/T_{sim}$ . The phase  $\varphi_i$  of each component was randomly chosen within the interval  $[0, 2\pi]$ , but to ensure the repeatability of the results a seed was used in the random number generator. An algorithm for energy conservation was applied to account for the power spectral density outside of the finite frequency range. The method, which is based on the ratio between the theoretical and the numerical zero-th moment of the spectrum, allows to generate a truncated JONSWAP spectrum with the same energy content of the continuous one.

The frequency dependent matrices of excitation and radiation force  $\mathbf{F}_e(\omega)$  and  $\mathbf{R}(\omega)$  were estimated by solving the scattering and radiation problems with the boundary element code AQWA (ANSYS Inc., USA). The simulations were performed for wave frequencies from 0.1 to 8 rad/s with a frequency step of 0.1 rad/s. Mesh convergence studies were performed to ensure grid independent solutions.

The electromagnetic force due to the PTO system  $\mathbf{F}_{PTO}(t)$  was calculated by dividing the three-phase electric power by buoy velocity and by generator efficiency  $\eta$ :

$$F_{PTO}(t) = \frac{\sum_{k=A,B,C} e_k(t) \cdot i_k(t)}{\eta \dot{z}(t)} \quad (5)$$

where  $i_k(t)$  is k-phase current and  $e_k(t)$  is k-phase electromotive force, calculated according to Faraday-Lenz laws:

$$e_k = -N_{ph} \frac{d\Phi_{Mk}(t)}{dt} \quad (6)$$

where  $N_{ph}$  is the number of windings for each phase and  $\Phi_{Mk}(t)$  is the magnet's flux linkage. Phase currents  $i_k(t)$  were calculated by solving the following ordinary differential equation (ODE) system:

$$\begin{aligned} e_A &= (R_c + R_l)i_A(t) + L \frac{di_A(t)}{dt} \\ e_B &= (R_c + R_l)i_B(t) + L \frac{di_B(t)}{dt} \\ e_C &= (R_c + R_l)i_C(t) + L \frac{di_C(t)}{dt} \end{aligned} \quad (7)$$

where  $R_C$  is coil resistance,  $R_l$  is load resistance and  $L$  is self-inductance. Generator parameters such as magnetic flux linkages and inductances were estimated by 2D finite element simulations of the linear generator [35].

The numerical integration of the coupled systems of differential equations (eq. 1 and eq. 7) was performed by the commercial code Matlab® using a 4<sup>th</sup> order Runge-Kutta scheme. Simulations were run for 1200 s. Once the equations were solved for buoy displacements and velocities and the instantaneous power of each unit was obtained, the mean power output was estimated by averaging the instantaneous power over the entire length of the simulation (neglecting an initial transient equal to the upper limit of the convolution integral of the radiation force). Finally, the mean power absorption of the array was obtained summing the power outputs of each unit.

### 3. Simulations

Wave farms of four units were simulated considering different configurations, i.e. different combinations of geometrical layout, distance between WECs and incident wave direction. Each buoy has diameter  $D$  equal to 4 m, height equal to 0.8 m and draft equal to 0.4 m. The nominal power of the linear generator was set equal to 10 kW. The array geometries are shown in Fig. 1. The first layout (a) represents a line of WECs, the second one (b) a square array and the last one (c) a rhombus array consisting of two equilateral triangles.

For each layout, four distances among the units were investigated: 20, 40, 80 and 120 m, i.e. 5, 10, 20 and 30  $D$ . The wave direction rose was discretized into 12 direction bins, every 30°. Taking into account the symmetries of the layouts, two wave directions were simulated for the square array and four for the linear and rhombus layouts (Table 1).

For each incident wave direction, 90 sea states were simulated, considering 9 significant wave height ( $H_S$ ) bins (from 0.25 m to 4.25 m at intervals of 0.5 m) and 10 peak periods ( $T_P$ ) ranging from 2.5 to 11.5 s at intervals of 1 s. The power output of the farms was calculated for each sea state to obtain the so-called power matrix, which contains the average power generated by the array as function of wave height and period.

### 4. Results: sensitivity of array performance to design parameters

The performance of a wave farm is commonly measured with the q-factor or interaction factor  $q$ , i.e. the ratio between the power output of an array of  $N$  units and the power output of  $N$  isolated units [3]. A q-factor larger than one means that the wave interactions have a positive effect on array power production and that constructive wave interferences lead to a power gain, as compared with the production of isolated systems. Conversely, when the interaction factor is lower than one, destructive wave interferences prevail and the park effect is negative.

Since array performance depends on wave period and much lesser on wave height [9], in this work the q-factor is calculated on the basis of the maximum power production of the array over the wave periods of the power production – averaged in the wave height space. Other choices were possible, such as considering the mean q-factor over the wave periods, as in De Andres et al. [11]. However, this criterion allows to focus on the most significant wave interactions, occurring around the wave period for which most of the power is produced, as outlined by Babarit [9]. Fig. 2 shows the q-factor of linear

(upper panel), square (central panel) and rhombus (lower panel) layouts as a function of non-dimensional distance between the units, for different wave incident directions. Dotted lines connecting the points are drawn as a guide for the eye only and they do not mean that linear interpolation is introduced. The thicker horizontal black line,  $q = 1$ , clearly distinguishes the cases of constructive ( $q > 1$ ) and destructive ( $q < 1$ ) wave interference.

The results indicate that some array configurations induce constructive wave interference while others have a negative effect on farm power output, in agreement with experimental results [36-38]. However, it is also evident that the effects of constructive and destructive interactions are generally limited, as observed in many previous studies. In the worst farm design, corresponding to a linear layout of very close units ( $d = 5D$ ) perpendicular to wave fronts, the maximum absorbed power is 20% less than four isolated devices. Nevertheless, in all the other cases, the reduction/increase in the maximum absorbed power with respect to isolated systems is less than 10%.

The results also illustrate the sensitivity of array performance to design parameters, i.e. geometrical layout, separating distance and wave direction. It can be noticed that the effect of wave direction and WEC distance depends on array geometry: linear layouts are influenced by both parameters, but not to the same extent, wave direction being the most important; square arrays are almost insensitive to the distance between the units and substantially only affected by wave direction and in rhombus layouts the performance is equally influenced by wave direction and separation distance.

Even if the effect of separating distance depends on array layout, all farm geometries have some common features, as observed in literature: (i) the behavior of the  $q$ -factor with respect to distance is typically not monotonic, because hydrodynamic interactions depend on the ratio between WEC distance and wavelength [9, 11], (ii) there is no optimal spacing between the units, but rather the best WEC distance should be selected as a function of the incident wave direction [9] and (iii) the effect of wave interactions is inversely proportional to the distance between the units and it is a few percents once the separating distance is larger than  $30 D$  [13].

#### 4.1 Linear layout

Focusing now on the specific characteristics of each array geometry, it can be noticed that in linear arrays wave interaction effects are strongest when the separation between the units is very small ( $5D$ ) and decay rapidly with distance, faster than in other layouts. Strong interactions within linear arrays with very closed units were already observed by Thomas et al. [39] in an experimental study on a linear wave farm of 5 heaving floats. In linear wave farms, strong masking effects occur for normal wave incidence ( $\beta = 90^\circ$ ), leading to destructive interferences for all the simulated distances. In this case, even at  $d = 30D$ , the maximum power absorbed by the array is 10% lower than the power output of four isolated WECs. Conversely, for parallel wave incidence ( $\beta = 0^\circ$ ) the park effect is negligible and the single units behave as isolated systems as long as they are separated by at least  $10D$ . For oblique wave attack angles ( $\beta = 30^\circ$  and  $\beta = 60^\circ$ ), wave interactions can be either positive or negative, depending on WEC distance. The linear layout which maximizes the  $q$ -factor is at  $\beta = 30^\circ$  (i.e. wave fronts at  $30^\circ$  to the row of devices) and separation distance equal to five buoy diameters ( $20 m$ ). This configuration would allow to increase the maximum power output by 12% with respect to the isolated systems. However, when the units are separated by only  $5D$ , strong destructive interferences occur for incident angles between  $60^\circ$  and  $90^\circ$ . Therefore, as real wave climates are

rarely unidirectional and positive wave interactions are much more limited than negative effects, it seems more advisable to design a linear wave farm in order to limit destructive interactions (mainly the normal wave incidence case) than to maximize positive effects. In this perspective, the optimum distance of separation of the units should be between  $10D$  and  $20D$ , because in this range the negative effects (at  $\beta = 90^\circ$ ) are much smaller (10% with respect to 20%) and a net power gain can be achieved for all the incident wave directions between  $0^\circ$  and  $60^\circ$ .

#### 4.2 Square layout

In square layouts the effect of the separating distance is negligible and the influence of the incoming wave direction is lower than in linear arrays, as already noticed by De Andrés et al. [11]. Due to the angular discretization by  $30^\circ$  intervals, only two layout orientations are possible, considering the double symmetry of the array geometry.

In first case ( $\beta = 0^\circ$ ) the wave farm consists in two lines of WECs parallel to wave fronts. In this configuration, the mutual interactions among the units have a negative effect on array power production, even at quite large separating distance ( $d = 30D$ ). However, the interaction factor is rather constant with respect to WEC distance, with an average value of 0.97. Previous experimental works on rectangular arrays refer to larger wave farms. For a rectangular array of 12 closely spaced ( $d = 2D$ ) heaving WECs, Weller et al. [37] found an average q-factor of 0.85, relatively constant over the entire range of tested frequencies. Stallard et al. [40] reported a mean interaction factor varying with wave period from 0.86 to 1.13, for a square array of 9 closely spaced ( $d = 2D$ ) heaving floats. It was observed both in numerical [13] and experimental studies [37, 40] that in a rectangular layout, even if the front units benefit from the waves radiated/diffracted by the rear units, this is not enough to compensate for the decrease in power absorption of the units in the back.

In the second case ( $\beta = 30^\circ$ ), the devices are arranged in four staggered rows, so that none of the units is shadowed by any other along the direction of wave propagation. This configuration allows to increase the maximum power absorbed by the array for all the separating distances, from 5 to 30 times the characteristic length of the WECs. However, in all the simulated square layouts the park effect is very small: for  $\beta = 30^\circ$  the maximum benefit by constructive wave interactions is 6% (with  $d = 10D$ ) while for  $\beta = 0^\circ$  the maximum reduction in the absorbed power is 5% (with  $d = 20D$ ). A similar result was reported in the experimental study of Stratigaki [41] on a 5x5 rectangular array of heaving WECs. The author found an increase in power production of 13% for a staggered layout with respect to a rectilinear layout. Concluding, in square arrays the distance between the units should not be a main issue and the farm design should rather focus on layout orientation, trying to ensure that the units are somewhat staggered in the direction of wave propagation

#### 4.3 Rhombus layout

Rhombus layouts are equally influenced by wave direction and separation distance. For  $\beta = 0^\circ$ , i.e. wave direction perpendicular to two sides of the rhombus, constructive wave interactions are achieved for separating distances up to  $30D$  with a maximum gain of 7% at  $d = 20D$ . This is the best orientation of the rhombus array because it allows to minimize destructive interferences (the devices are nearly unmasked) and to benefit from constructive interferences due to the radiated waves.



It is noteworthy to compare the rhombus layout for  $\beta = 0^\circ$  with the square array for  $\beta = 30^\circ$ . The q-factors of these configurations exhibit a very similar pattern: they are always higher than one and they have a convex shape. However, in the staggered square the positive effect is much smaller and decays faster with distance. Looking now at the arrangement of the devices with respect to incoming waves, it turns out that both the layouts are staggered in the direction of wave propagation but only the square layout is staggered in the direction normal to incident waves. This result could suggest that wave interferences are more beneficial when pairs of devices are aligned along the same wave front (rhombus array with  $\beta = 0^\circ$ ) so that the two units are in phase with each other.

With respect to  $\beta = 0^\circ$ , the other rhombus orientations are more affected by wake effects, because they have at least one pair of units aligned with the incident wave direction. When  $d = 10D$ , all the rhombus arrays exhibit a gain in power production around 5% with respect to four isolated units.  $\beta = 90^\circ$  is the worst case in terms of q-factor because two pairs of devices are parallel to wave direction. For this wave attack angle, the park effect is negative for both  $d = 20D$  (4% power loss) and  $d = 30D$  (3% power loss).  $\beta = 30^\circ$  or  $\beta = 120^\circ$  are better solutions because they have just one pair of devices aligned along the incident wave direction. In the first case, i.e. wave direction aligned with the shortest diagonal, the performance of the array is lower because due to the short distance between the two units parallel to wave direction masking effects are stronger. To conclude, in the design of rhombus arrays, care must be taken to avoid masking effects, due to the alignment of the devices with the direction of wave propagation, as resulting from the experiments by Stratigaki [41]. Particularly, the  $\beta = 90^\circ$  layout orientation resembling the square array with  $\beta = 0^\circ$  should be avoided, because two lines of WECs are aligned perpendicular to wave fronts, leading to two masked units. Finally, it is interesting to notice that the rhombus array is the only one characterized by an optimum distance among the units ( $d = 10D$ , regardless the orientation of the layout).

## 5. Application to real wave climates

### 5.1 Method

The power matrices of the different array configurations (i.e. combinations of layout geometry, WEC distance and wave direction) were used to identify the optimal wave farm designs for four locations off the Italian coasts. More specifically, the aim was to find out the most productive wave farm configuration, i.e. the one providing the highest annual energy output (AEO), at each study site. For this purpose, it was considered that each array layout can be deployed with different absolute orientations (with respect to north). According to the array's simulations computed with different incident wave angles (30 apart, see Section 3), six geographical deployment orientation are possible for linear and rhombus layouts and three for the square one (Fig. 3). Each oriented layout was also simulated considering four different distances between units, thus leading to 60 wave farm designs for each site.

The annual electricity production of a wave energy converter is estimated by multiplying the expected power output of a sea state (defined by  $H_S$ ,  $T_p$  pairs) by its occurrence (in hours) and then by summing over all the sea states. The same procedure is typically used for wave farms, assuming only one direction of propagation of the incident waves. In this work, instead, wave directionality is taken into account, assuming 12 directions of wave propagation, as explained above. As a result, the above

procedure was modified to account for wave directionality: for wave each direction, the probability of occurrence  $WC(i, j)$  of the sea state  $(i, j)$  was multiplied by the corresponding power matrix  $PM(i, j)$ , taking into account the direction of wave propagation with respect to the oriented layouts. Then, the annual energy production of the farm was obtained by summing the energy production over all the twelve wave directions. As an example, the annual energy production of a square layout  $S_\alpha$ , oriented with an angle  $\alpha$  with respect to north (see Fig. 3) was calculated by:

$$AEO(S_\alpha) = \sum_i^{N_H} \sum_j^{N_T} PM_0(i, j) [WC_\alpha(i, j) + WC_{90^\circ+\alpha}(i, j) + WC_{180^\circ+\alpha}(i, j) + WC_{270^\circ+\alpha}(i, j)] \\ + PM_{30^\circ}(i, j) [WC_{30^\circ+\alpha}(i, j) \\ + WC_{60^\circ+\alpha}(i, j) + WC_{120^\circ+\alpha}(i, j) + WC_{150^\circ+\alpha} + WC_{210^\circ+\alpha} + WC_{240^\circ+\alpha}(i, j) \\ + WC_{300^\circ+\alpha}(i, j) + WC_{330^\circ+\alpha}(i, j)]$$

where  $N_H$  and  $N_T$  denote the number of wave height and wave period bins.

## 5.2 Wave climate characterization

Recent assessments of wave energy potential in the Mediterranean Sea have shown that among the Italian seas some promising areas exist for wave energy exploitation [42-44]. The study sites selected for the present study (Alghero, Mazara, Ponza, La Spezia) are the four most energetic Italian locations where wave recording buoys are deployed. Most of them are located in the Tyrrhenian Sea, due to the longer fetches (Fig. 4), while Alghero is in the North-West of Sardinia, exposed to winter storms from Lion's gulf. The average annual wave power is 9.1 kW/m at Alghero, 4.7 kW/m at Mazara del Vallo, 3.7 kW/m at Ponza and 3.5 kW/m at La Spezia [45]. For each location, Fig. 5 shows annual sea state occurrences (left panel) and wave direction occurrences (right panel) based on 15 years of wave measurements of the Italian wave metric network [46]. Red numbers indicate the percentage of annual events falling into each wave direction bin, accordingly to the discretization of the wave direction data.

Wave climate data show that the prevailing sea states are characterized by relatively small waves. At Alghero and Mazara del Vallo, sea states with waves lower than 1 m (characterized by power levels in the range 2 – 4 kW/m) account for 60% of the year, while at the other locations, they account for 70%–80% of the time [42,43]. The peak period with the highest probability of occurrence is between 4.5 and 5.5 s at all locations. This means that the natural period of oscillation of a point absorber should be around 5 s in order to maximize the power output for the Italian wave climate. The occurrence matrix of Alghero is the most disperse with several extreme events, while Ponza is characterized by the most concentrated occurrence matrix.

Regarding energy distribution among sea states, at Alghero and La Spezia the available wave energy is split between two clusters of sea states. Moreover, at Alghero a relevant part of the annual energy is associated with highly energetic but rare events: more than 40% of the available resource is due to sea states with 4% of probability of occurrence. Differently, at Mazara del Vallo and Ponza the energy distribution is unimodal and the resource is more concentrated, in terms of both wave period and wave height. These differences in wave energy distribution are important for the performance of a wave energy converter and explain most of the differences found in the power production of a single unit among the study locations.

With regard to the directional occurrence of sea states, it can be noticed that the wave climate is fairly unidirectional at Alghero and La Spezia, bidirectional at Mazara del Vallo and multidirectional at Ponza. Alghero is dominated by waves coming from West and North-West quadrant, while at La Spezia most of the events are due to winds blowing from South and South-West. At Mazara del Vallo, the most frequent events come from West and South-East while at Ponza many directions are probable, from North-West to South-West.

### 5.3 Results

Figs. 6, 7 and 8 show the annual energy production of linear, square and rhombus arrays, respectively, as a function of WEC distance, for different layout orientations and for four isolated WECs (black dashed line). Each plot refers to a different location: (a) Alghero, (b) Mazara del Vallo, (c) Ponza and (d) La Spezia. The results clearly indicate that it is possible to find several array configurations, which perform slightly better than four isolated devices, at all the study sites. More specifically, the percentage of wave farms characterized by a q-factor higher than one is 47% at Alghero and La Spezia, 50% at Mazara del Vallo and 51% at Ponza, considering all the studied configurations. Therefore, even in bidirectional and multidirectional wave climates, such as Mazara del Vallo and Ponza, respectively, there exist a large number of arrays configurations which can absorb more energy than four isolated devices. This result differs from the current view (based on theoretical studies in unidirectional waves) that only in unidirectional, or almost unidirectional wave climates, constructive wave interactions would be possible [13, 24, 25] and it shows the importance of site-specific array optimization.

The results show that constructive wave interference can be achieved by all the layout geometries as long as the arrays are deployed with the appropriate orientation. However, rhombus layouts can more easily benefit from constructive interaction effects: 57% of the rhombus arrays are characterized by higher power absorption than four isolated WECs, against 48% of linear layouts and 42% of square layouts.

Separating distance seems to be a key factor in achieving constructive interactions. Almost all the curves arrange in a convex shape, with a significant drop in energy production for WEC spacing larger than 20D. The highest power gain is achieved when the distance among the units falls in the range between 10 and 20 buoy diameters. An exception is represented by the linear layout, which has the highest productivity for very close units (i.e. 5 diameters of separation distance). Conversely, all the rhombus and square layouts are characterized by destructive wave interferences when the units are very close.

The results allow to find the wave farm configurations which maximize the annual energy production at each study site. Optimal designs are reported in Figure 9, together with the expected values of power gain, with respect to the isolated WECs. The figure also reports the array configurations minimizing the absorbed power and the associated values of power loss. The results are divided by array geometry because it is likely that the choice of the layout geometry is constrained by other issues related, for example, to the mooring system, the sea area use, the environmental impact.

At Alghero, the array design maximizing the annual energy production corresponds to a rhombus layout with a WEC distance of 20D. The rhombus should be oriented so that the devices are arranged in two rows perpendicular to the prevailing wave direction (i.e. 300°) and staggered along the direction

of the incoming sea (i.e. orientation R60). Assuming a single wave direction equal to the prevailing one, this orientation would correspond to the  $\beta = 0^\circ$  case of Fig. 2c, i.e. the optimum rhombus orientation in unidirectional seas. Notably, the best performance is not provided by the linear array, even if the wave climate is nearly unidirectional. This is due to the fact that in a staggered grid, the first row benefits from constructive interactions due to the waves radiated by the units behind and the second row, which is nearly unmasked, benefits from radiation, as well [10]. Finally, it is worthwhile to notice that the wave farm design R60 with  $d = 20D$  is a robust solution, with respect to small changes in layout orientation and WEC distance, which are quite probable due to model uncertainties and inaccuracies in array deployment. In fact, if the layout orientation is modified by  $\pm 30^\circ$  (i.e. R30 or R90) or the distance among the units is changed by  $\pm 10D$ , the layout still benefits from positive wave interactions.

At Mazara del Vallo, Ponza and La Spezia, the highest energy production is obtained by a linear layout and very close units ( $d = 5D$ ). In all the three sites, the line of WECs should be oriented at  $60^\circ$  to the dominant direction of wave propagation. This agrees with the results obtained in unidirectional seas, showing that the  $60^\circ$  incidence (corresponding to  $\beta = 30^\circ$  case in Fig. 2a) is the most efficient wave direction in linear layouts. Differently from Alghero, now the optimum array designs are not robust with respect to perturbations of the wave attack angle. Especially at Ponza and La Spezia the wave farms perform quite poorly when the wave direction changes by  $\pm 30^\circ$  with respect to the optimal direction. This is due to the fact that linear arrays are the most sensitive to wave direction, particularly for small separating distances.

Finally, it is important to focus on the values of energy gain and loss associated to the designs, which maximize and minimize, respectively, the annual energy output. It is evident that the effect of wave interactions on absorbed power is quite low, as already observed in previous studies on small wave farms [13]. The best arrays designs lead to an energy gain of about 1% at Alghero, and about 3% in the other locations and the worst array designs lead to a decrease in energy production of 5% at La Spezia and 6% in the other sites. As a result, the difference in the annual energy output between the best and worst array configuration is rather small, between 7% and 9%, depending on the deployment location. Moreover, it is worthwhile to consider how the results change if the  $5D$  distance among the units is not taken into account (as suggested by Bogarino et al. [10], such short distance is not likely to occur, due to mooring, operation and maintenance issues). Allowing only for distances higher than  $10D$ , the maximum gain in energy production reduces to 2%, the maximum loss to 3% and the overall park effect to 5%, considering all the deployment sites and all the studied configurations.

## 6. Discussion and conclusions

In this work the effects of wave interactions in arrays of point absorbers, hypothetically deployed at some Italian locations, has been investigated. The analysis has fully taken into account real wave conditions, particularly intra-annual wave direction variability. In this way, a site-specific optimization has been carried out for the selected Italian locations and new insights have been provided for wave farm design in real wave climates. The main findings of the work can be summarized as follows:

- Array performance is affected by both the arrangement of the units within the array (i.e. layout geometry and distance among the units) and the direction of incoming sea, as already observed (e.g. [11, 12]). The effect of wave direction and WEC spacing depend on park geometry: linear and

rhombus arrays are influenced by both wave direction and separating distance while square layouts are mostly affected by wave direction.

- In unidirectional seas, wave farms should be deployed according to the following indications: WEC lines should stay at  $30^\circ$  with respect to wave fronts, square arrays should avoid the alignment between wave direction and square sides and rhombus layout should be oriented so that the two rows are parallel to wave fronts.
- The distance among the units plays a key role in array performance. Too close or too spaced units can hardly benefit of constructive wave interferences, as already observed by Singh and Babarit [14]. The optimum distance is between 10 and 20 buoy diameters.
- Array configurations which allow to increase the energy production with respect to isolated units, are possible both in theoretical unidirectional wave fields and in real multidirectional wave climates. More specifically, it is possible to design a four WECs farm off the Italian coasts, which performs better than four isolated devices, taking advantage of constructive wave interferences. This result is of utmost interest for WEC array designers and contradicts the present view that destructive interactions would be prevailing in real wave climates [13, 24, 25] thus showing the importance of site-specific array optimization.
- The optimum array designs for the studied locations are the following: a rhombus layout with WEC distance equal to  $20D$  at Alghero and a linear layout with  $5D$  spacing at the other locations. In all the sites, the layouts should be oriented by aligning the most productive wave farm orientation with the prevailing wave direction. In other words, the optimum array orientation can be assessed as if the waves were coming by one direction, equal to the prevailing one.
- The optimum wave farm designs lead to power gains from 1.5 % (at Alghero) to 3.4 % (at Mazara del Vallo). More generally, the effects of constructive and destructive wave interactions are quite limited as noticed in previous analysis in unidirectional seas (Babarit, 2013). The difference in energy production between the most and least favorable configuration ranges between 3% and 9% depending on array geometry and deployment location. This difference further decreases if WEC distances lower than  $10D$  are not considered, due to likely mooring constraints [10]. In that case, the difference in energy production between the best and worst array design drop to 5%, at maximum.
- In conclusion, for the selected Italian locations, the effect of wave interactions on energy absorption is not expected to be a main issue, as long as the devices are separated by at least 10 buoy diameters and that the layouts are oriented to achieve the maximum energy absorption for the prevailing wave direction.

In this work, the maximization of the annual energy production was considered as the main goal. However, arrays design is not a single objective optimization problem. Hydrodynamic and electric interaction between park units have also an important effects on power fluctuations. As well as power magnitude, power variance also depends on park geometry, distance of separation between units and incoming wave direction. Previous studies (e.g. [15, 47]) showed that except for the linear layout parallel to wave fronts, all other wave farm designs allow to significantly reduce power fluctuations. Other issues that must be considered are the mooring system layout [8], installation and maintenance costs, electrical configuration [23], environmental impact and occupation of the ocean area [48].

Finally, it is important to stress that the results of the present work refer to a small array. According to previous studies (e.g. [10, 12]), constructive wave interactions would not be probably attained in larger wave farms.

## References

- [1] Day AH, Babarit A, Fontaine A, He YP, Kraskowski M, Murai M et al. Hydrodynamic modelling of marine renewable energy devices: A state of the art review. *Ocean Eng.* 2015;108:46–69.
- [2] Folley M, Babarit A, Child B, Forehand D, O’Boyle L, Silverthorne K et al. A review of numerical modelling of wave energy converters arrays. In: *Proc. 31<sup>st</sup> International Conference on Ocean, Offshore and Arctic Engineering*; 2012.
- [3] Budal K. Theory of absorption of wave power by a system of interacting bodies. *J. Ship Res.* 1977;21:248–53.
- [4] Evans DY. Some analytical results for two and three dimensional wave-energy absorbers. In: *Power from Sea Waves*, London: Academic Press; 1980.
- [5] Simon MJ. Multiples scattering in arrays of axisymmetric wave-energy devices - a matrix method using a plane-wave approximation. *J. Fluid Mech.* 1982;120:1–25.
- [6] McIver P. Wave forces on arrays of floating bodies. *J. Eng. Math.* 1984;18:273–85.
- [7] Cruz J, Sykes R, Siddorn P, Taylor R. Estimating the loads and energy yield of arrays of wave energy converters under realistic seas. *IET Renew. Power Gen.* 2010;4:488–97.
- [8] Vicente PC, de O. Falcão AF, Gato LMC, Justino PAP. Dynamics of arrays of floating-point absorber wave energy converters with inter-body and bottom slack-mooring connections. *Appl. Ocean Res.* 2009;31:267–81.
- [9] Babarit A. Impact of long separating distances on the energy production of two interacting wave energy converters. *Ocean Eng.* 2010;37:718–29.
- [10] Borgarino B, Babarit A, Ferrant P. Impact of wave interactions effects on energy absorption in large arrays of wave energy converters. *Ocean Eng.* 2012;41:79–88.
- [11] de Andrès AD, Guanche R, Meneses L, Visal C, Losada JJ. Factors that influence array layout on wave energy farms. *Ocean Eng.* 2014;82:32–41.
- [12] Göteman M, Engström J, Eriksson M, Isberg J, Leijon M. Methods of reducing power fluctuations in wave energy parks. *J. Renew. Sustain. Ener.* 2014;6:043103.
- [13] Babarit A. On the park effect in arrays of oscillating wave energy converters. *Renew. Energy* 2013;58:68–78.
- [14] Singh J, Babarit A. A fast approach coupling Boundary Element Method and plane wave approximation for wave interaction analysis in sparse arrays of wave energy converters. *Ocean Eng.* 2014;85:12–20.
- [15] Göteman M, Engström J, Eriksson M, Isberg J. Optimizing wave energy parks with over 1000 interacting point-absorbers using an approximate analytical method. *Int. J. Mar. Energy* 2015;10:113–26.
- [16] Falnes J. Radiation impedance matrix and optimum power absorption for interacting oscillators in surface waves. *Appl. Ocean Res.* 1980;2:75–80.

- [17] Child B, Venugopal V. Interaction of waves with an array of floating wave energy devices. In: Proc. 7<sup>th</sup> European Wave and Tidal Energy Conference; 2007.
- [18] Michele S, Sammarco P, d'Errico M, Renzi E, Abdolali A, Bellotti G et al. Flap gate farm: from Venice lagoon defense to resonating wave energy production. Part2: Synchronous response to incident waves in open sea. *Appl. Ocean Res.* 2015;52:43–61.
- [19] Engström J, Eriksson M, Göteman M, Isberg J, Leijon M. Performance of a large array of point-absorbing direct-driven wave energy converters. *J. Appl. Phys.* 2013;114:204502.
- [20] Bacelli G, Ringwood JV. Constrained control of arrays of wave energy devices. *Int. J. Mar. Energy* 2013;3–4:53–69.
- [21] Garcia Rosa P, Bacelli G, Ringwood JV. Control-informed optimal array layout for wave farms. *IEEE Trans. Sustain. Energy* 2015;6:575–82.
- [22] Nambiar AJ, Forehand DIM, Kramer MM, Hansen RH, Ingram DM. Effects of hydrodynamic interactions and control within a point absorber array on electrical output. *Int. J. Mar. Energy* 2015;9:20–40.
- [23] Sharkey F, Bannon E, Conlon M, Gaughan K. Maximising value of electrical networks for wave energy converter arrays. *Int. J. Mar. Energy* 2013;1:55–69.
- [24] Fitzgerald C, Thomas G. A preliminary study on the optimal formation of an array of wave power devices. In: Proc. 7<sup>th</sup> European Wave and Tidal Energy Conference; 2007.
- [25] Thomas G. Some observations on modelling arrays of wave power devices. In: Slideshow of presentation at NUIM wave energy workshop, Maynooth, Ireland; 2011.
- [26] Leijon M, Waters R, Rahm M, Svensson O, Boström C, Strömstedt E et al. Catch the wave to electricity: the conversion of wave motions to electricity using a grid-oriented approach, *IEEE Power Energy Mag.* 2009;7(1):50–4.
- [27] Lejerskog E, Boström C, Hai L, Waters R, Leijon M. Experimental results on power absorption from a wave energy converter at the Lysekil wave energy research site. *Renew. Energy* 2015;77:9–14.
- [28] Bozzi S, Moreno Miquel A, Antonini A, Passoni G, Archetti A. Modeling of a point absorber for energy conversion in Italian seas. *Energies* 2013;6:3033–51.
- [29] Bozzi S, Moreno Miquel A, Scarpa F, Antonini A, Archetti R, Passoni G et al. Wave energy production in Italian offshore: preliminary design of a point absorber with tubular linear generator. In Proc. International Conference on Clean Electrical Power; 2013.
- [30] Miquel AM, Antonini A, Archetti R, Bozzi S, Passoni, G. Assessment of the surge e effects in a heaving point absorber in the Mediterranean sea. In: Proc. 33<sup>rd</sup> International Conference on Ocean, Offshore and Arctic Engineering; 2014.
- [31] Cummins W. The impulse response function and ship motions. *Schiffstechnik* 1962;9:101–9.
- [32] Jefferys ER. Device characterization. In: Count B, editor. *Power from Sea Waves*, London: Academic Press; 1980, p. 413–38.
- [33] De O. Falcão AF. Modelling and control of oscillating body wave energy converters with hydraulic power take off and gas accumulator. *Ocean Eng.* 2007;34:2021–32.
- [34] APAT. *Atlante delle onde nei mari italiani - Italian wave atlas*, Roma; 2004.
- [35] Bizzozero F, Giassi M, Gruosso G, Bozzi S, Passoni G. Dynamic model, parameter extraction, and analysis of two topologies of a tubular linear generator for seawave energy production. In:

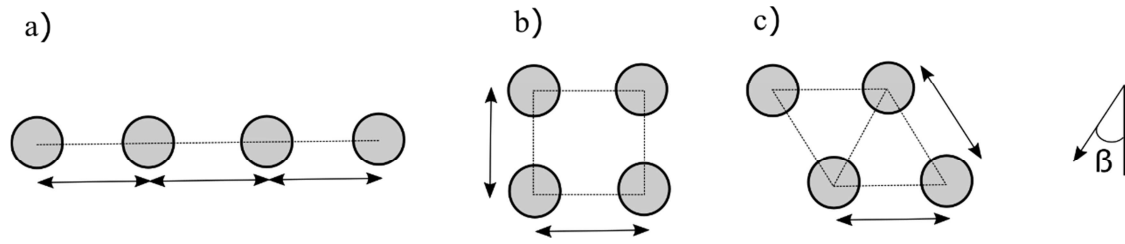
Proc. 22<sup>nd</sup> International Symposium on Power Electronics, Electrical Drives, Automation and Motion; 2014.

- [36] Ashton I, Johanning L, Linfoot B. Measurement of the effect of power absorption in the lee of a wave energy converter. In: Proc. 28<sup>th</sup> International Conference on Offshore Mechanics & Arctic Engineering; 2009.
- [37] Weller S, Stallard T, Stansby PK. Experimental measurements of irregular wave interaction factors in closely spaced arrays. In: Proc. 8<sup>th</sup> European Wave and Tidal Energy Conference; 2009.
- [38] Stratigaki V, Troch P, Stallard T, Forehand D, Kofoed JP, Folley M et al. Wave basin experiments with large wave energy converter arrays to study interactions between the converters and effects on other users in the sea and the coastal area. *Energies* 2014;7:701-34.
- [39] Thomas S, Weller S, Stallard TJ. Float response within an array: numerical and experimental comparison. In: Proc. 2<sup>nd</sup> International Conference on Ocean Energy; 2008.
- [40] Stallard T, Stansby PK, Williamson A. An experimental study of closely spaced point absorber arrays. In: Proc. 18<sup>th</sup> International Offshore & Polar Engineering Conference; 2008.
- [41] Stratigaki V. Experimental study and numerical modelling of intra-array interactions and extra-array effects of wave energy converter arrays. Ph.D. dissertation, Ghent University; 2014.
- [42] Archetti R, Bozzi S, Passoni G. Feasibility study of a wave energy farm in the western Mediterranean sea: comparison among different technologies. In: Proc. 30<sup>th</sup> International Conference on Ocean, Offshore and Arctic Engineering; 2011.
- [43] Bozzi S, Archetti R, Passoni G. Wave electricity production in Italian offshore: A preliminary investigation. *Renew. Energy* 2014;62:407–16.
- [44] Besio G, Mentaschi L, Mazzino A. Wave energy resource assessment in the Mediterranean sea on the basis of a 35-year hindcast. *Energy* 2006;94:50–63.
- [45] Vicinanza D, Cappietti L, Ferrante V, Contestabile P. Estimation of the wave energy in the Italian offshore. *J. Coast. Res.* 2011;64:613–17.
- [46] ISPRA Idromare website. [Online]. Available: <http://www.idromare.it/>
- [47] Bizzozero F, Bozzi S, Gruosso G, Passoni G, Giassi M. Spatial interactions among oscillating wave energy converters: electricity production and power quality issues. In: Proc. 42<sup>nd</sup> Annual Conference of IEEE Industrial Electronics Society; 2016.
- [48] Palha A, Mendes L, Juana Fortes C, Brito-Melo A, Sarmiento A. The impact of wave energy farms in the shoreline wave climate: Portuguese pilot zone case study using Pelamis energy wave devices. *Renew. Energy* 2010;35:62–77.

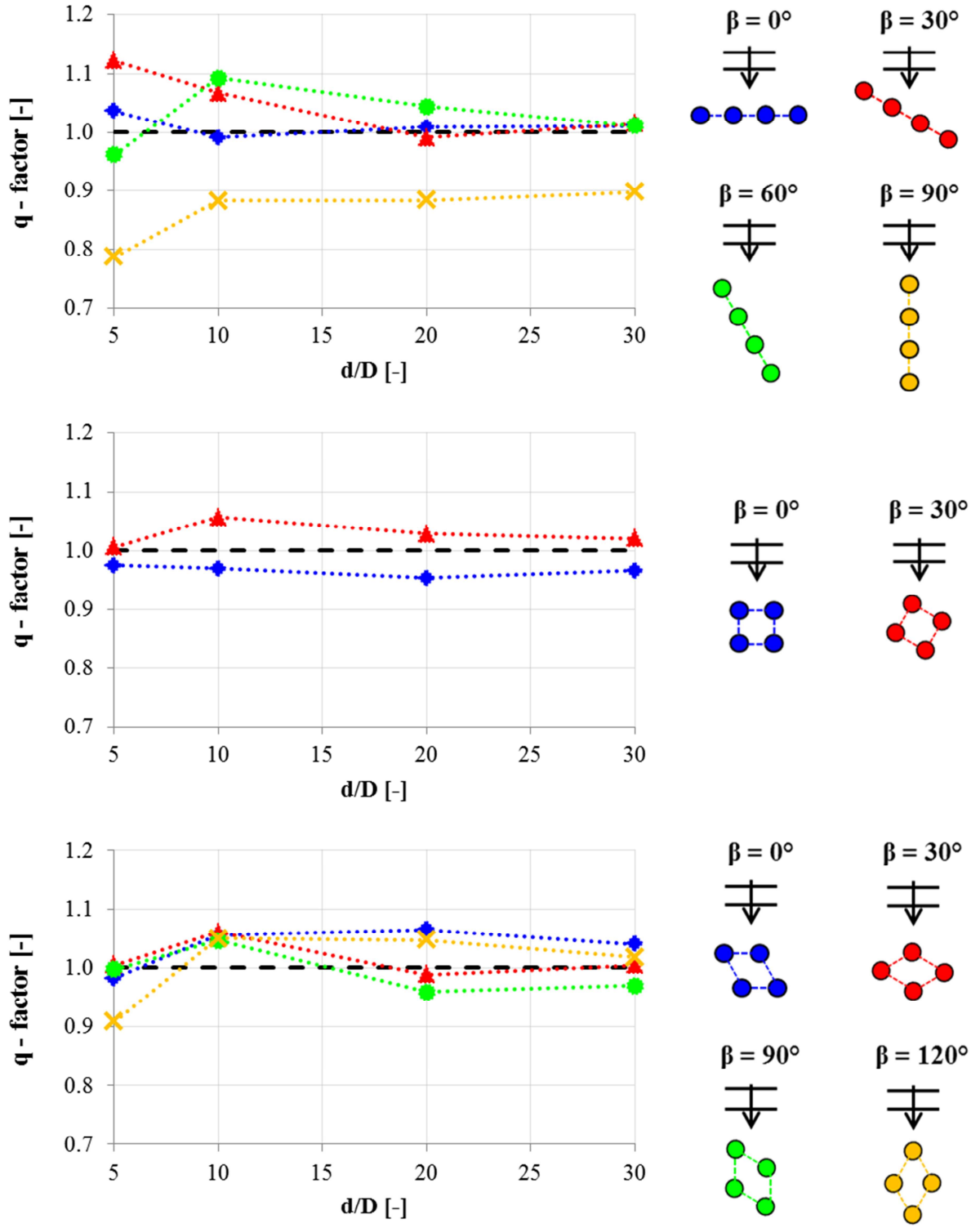


**Table 1.** Simulated wave directions (°) of each geometrical layout.  
Equivalent wave directions, in terms of array power production are reported in parenthesis.

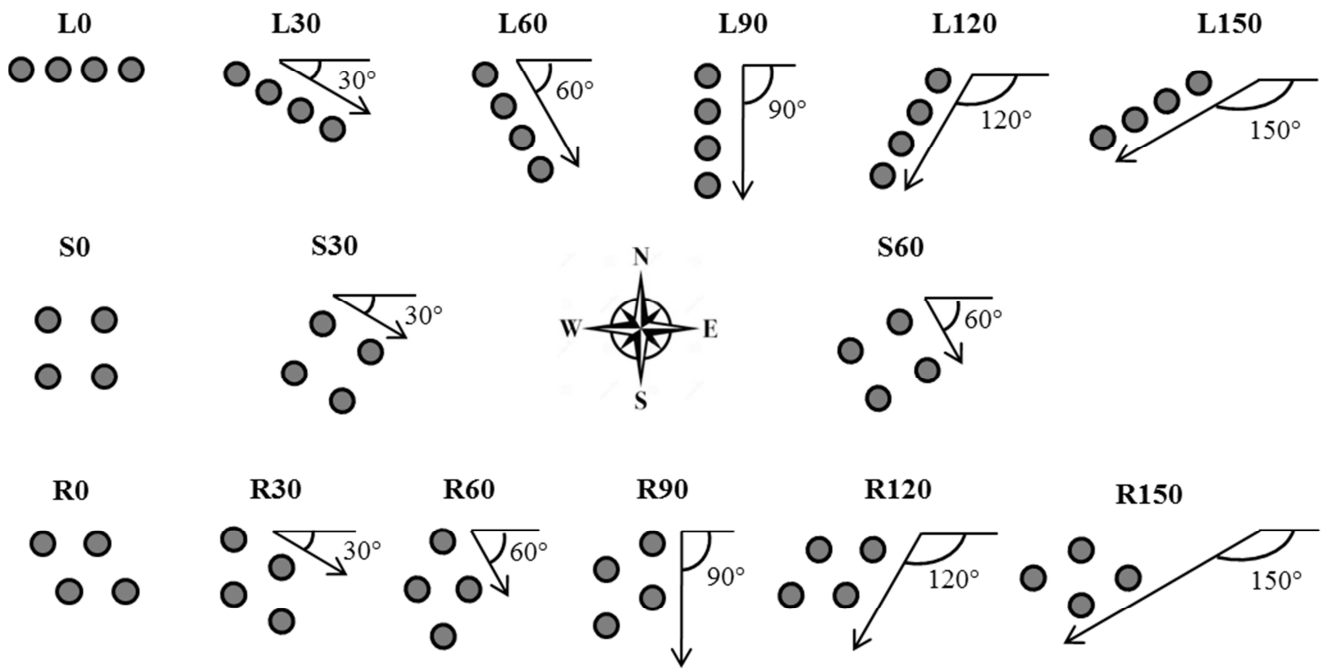
<b>Linear</b>	<b>Square</b>	<b>Rhombus</b>
<b>0°</b> (180°)	<b>0°</b> (90°, 180°, 270°)	<b>0°</b> (60°, 180°, 240°)
<b>30°</b> (150°, 210°, 330°)	<b>30°</b> (60°, 120°, 150°, 210°, 240°, 300°, 330°)	<b>30°</b> (210°)
<b>60°</b> (120°, 240°, 300°)		<b>90°</b> (150°, 270°, 330°)
<b>90°</b> (270°)		<b>120°</b> (300°)



**Figure 1.** Simulated array layouts: (a) linear, (b) square and (c) rhombus.



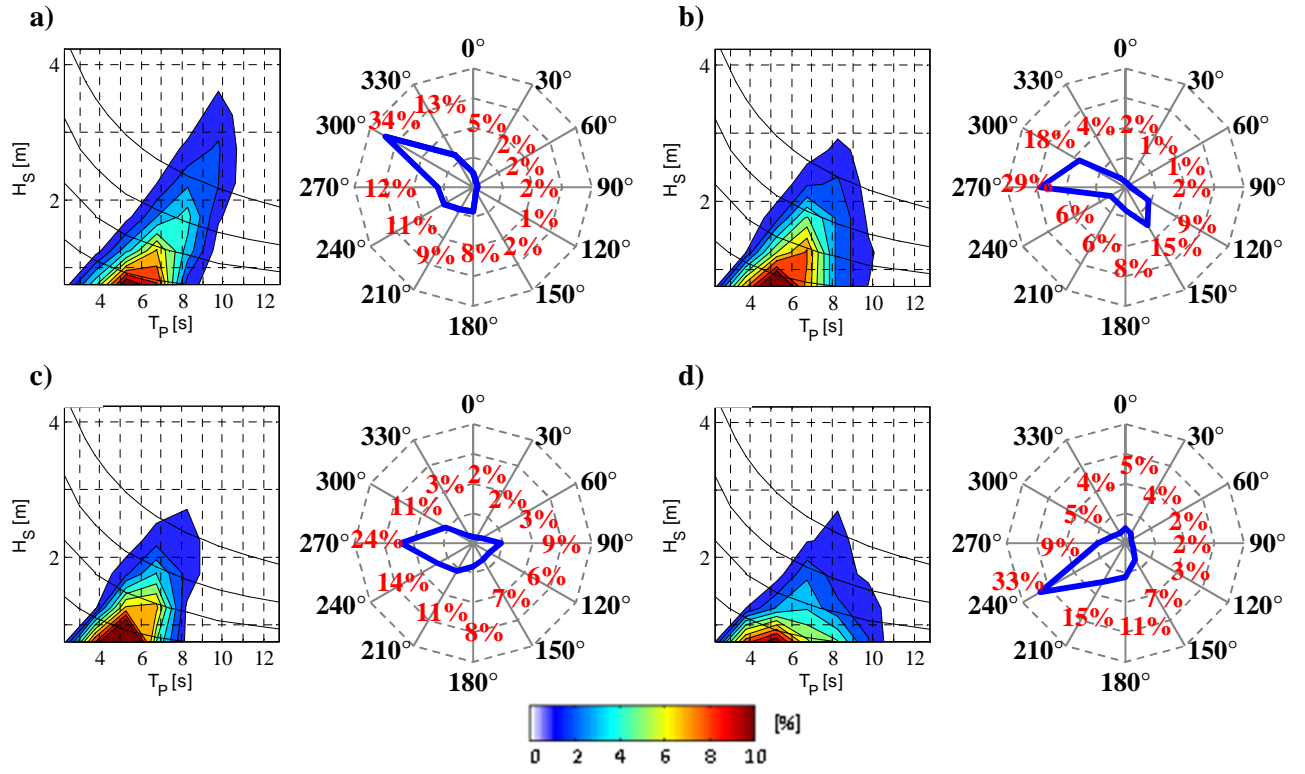
**Figure 2.** q-factor of linear (upper panel), square (central panel) and rhombus (lower panel) layouts as a function of non-dimensional distance among the units, for different wave incident directions.



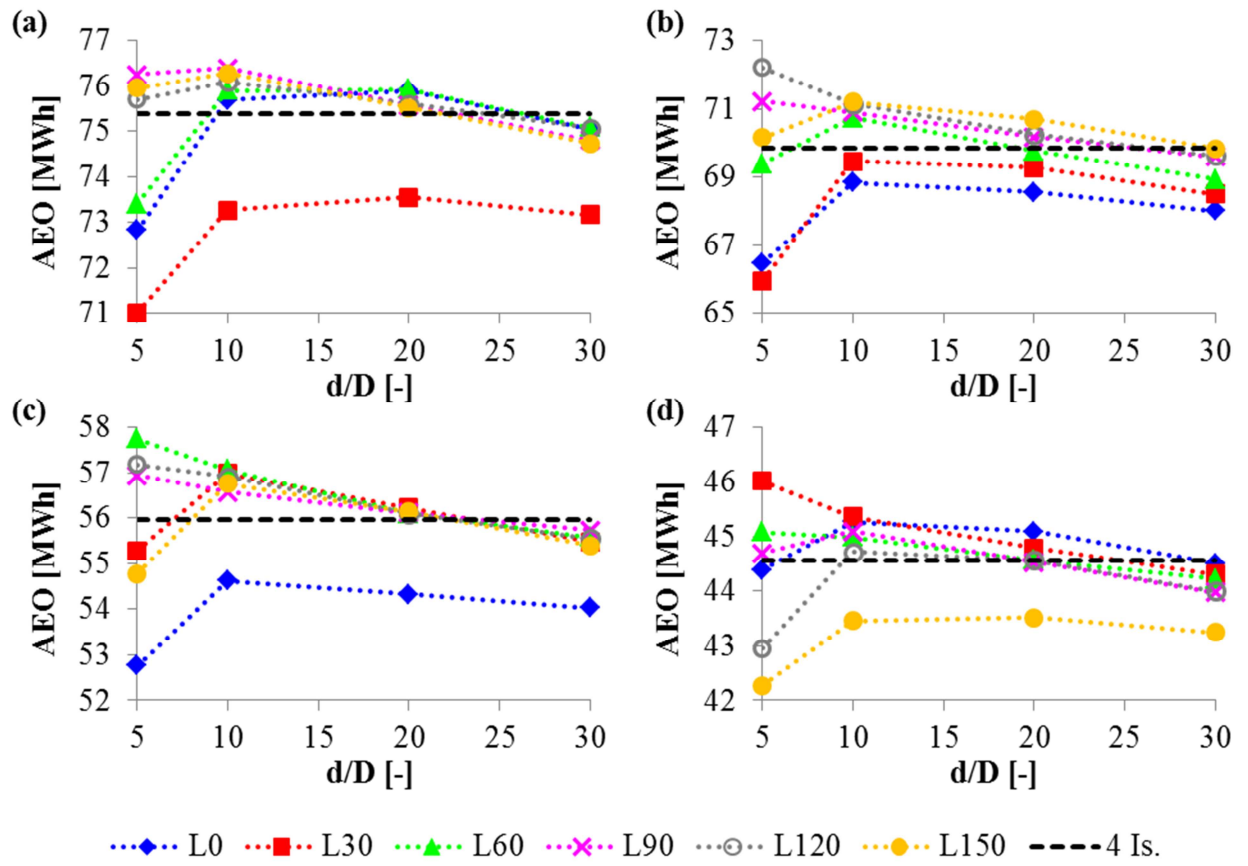
**Figure 3.** Layout orientations simulated at each study site.



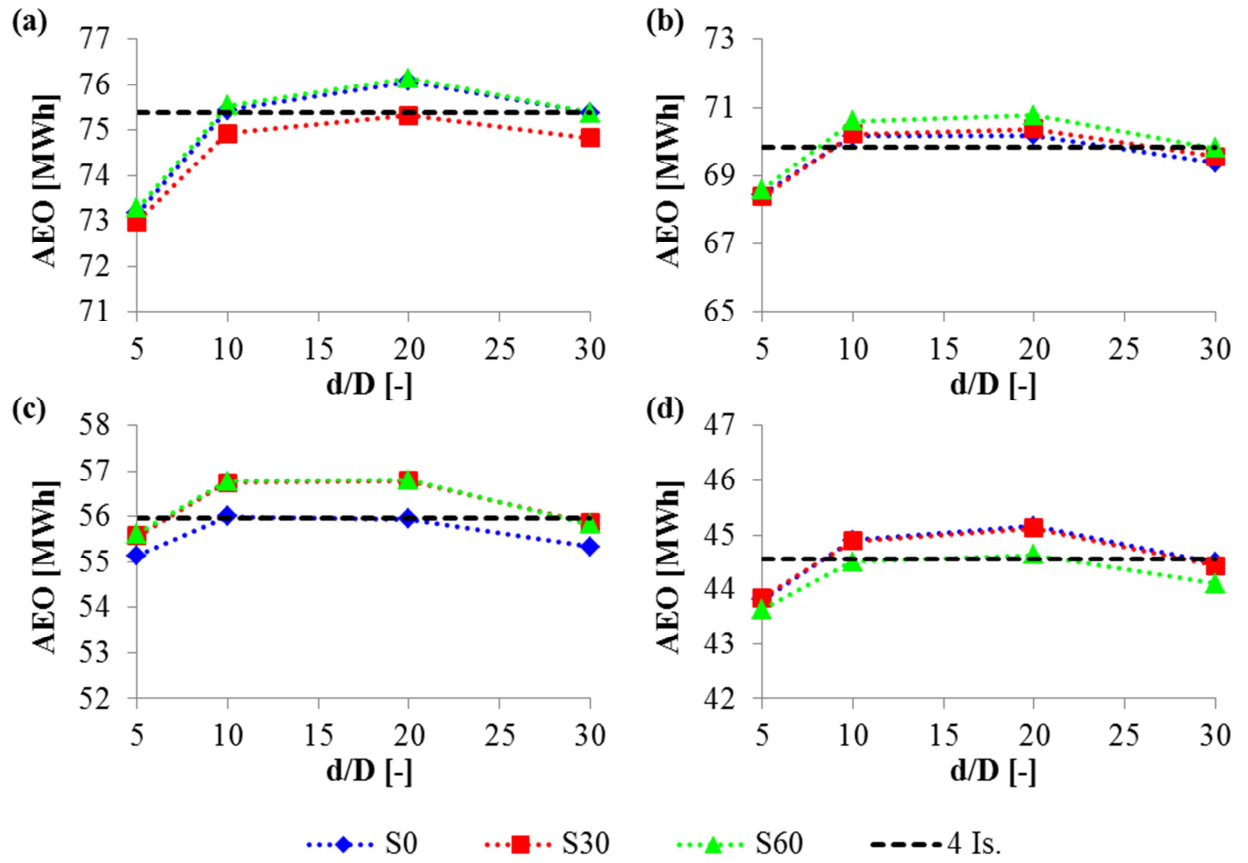
**Figure 4.** Location of the study sites.



**Figure 5.** Wave climate of the study sites: (a) Alghero, (b) Mazara del Vallo, (c) Ponza and (d) La Spezia. Left plots show sea state occurrences (%) and right plots report wave direction occurrences (%). Red numbers in rose plots indicate the percentage of annual events falling into each wave angle bin.

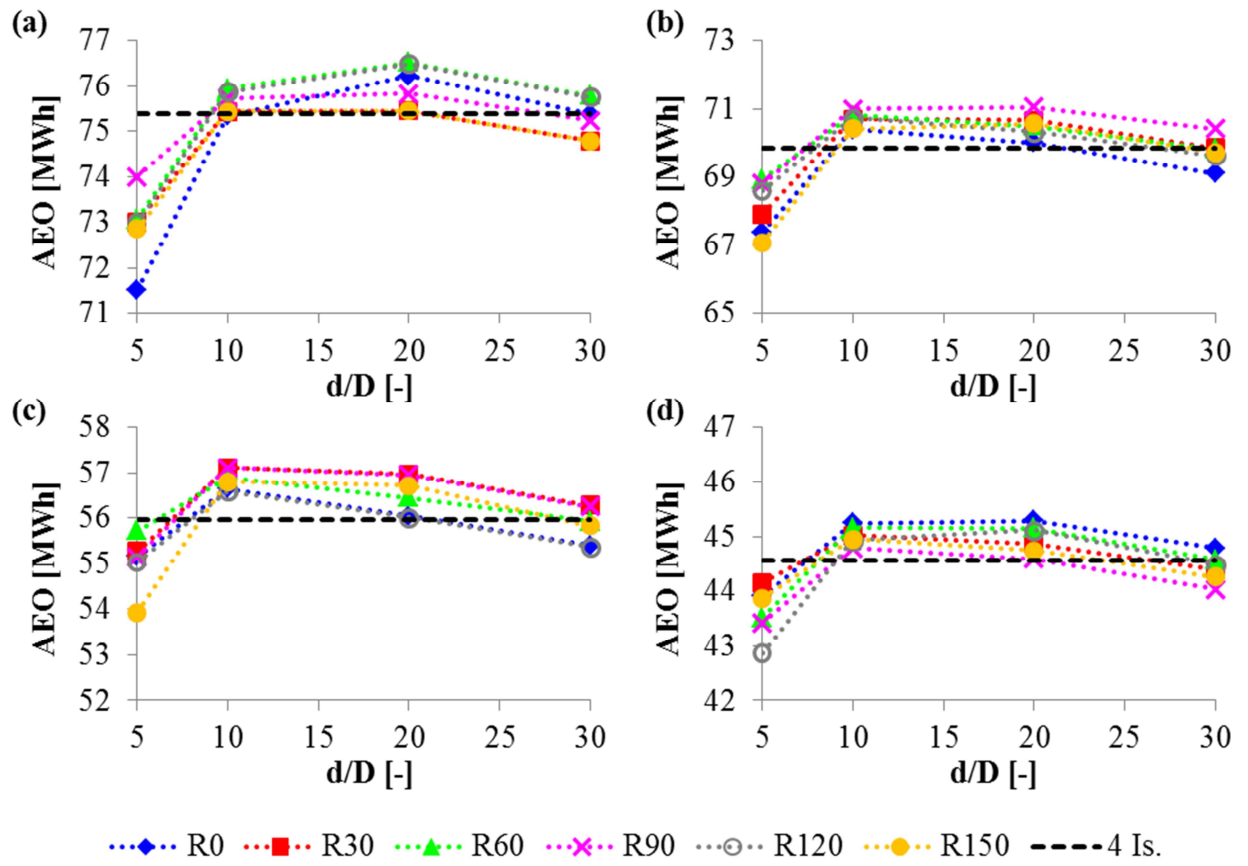


**Figure 6.** Annual energy production (AEO) as a function of WEC distance for linear arrays with different orientations: (a) Alghero, (b) Mazara del Vallo, (c) Ponza and (d) La Spezia. Black lines represent AEO of four isolated WECs.

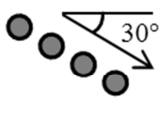

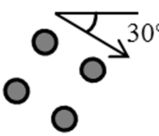
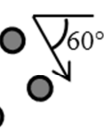

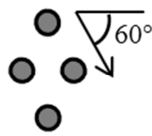
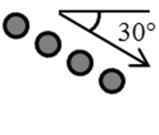

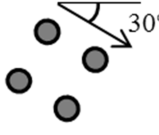
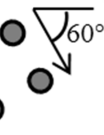
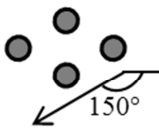
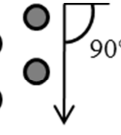

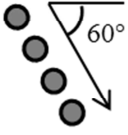

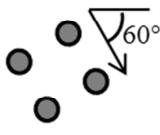
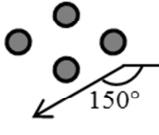
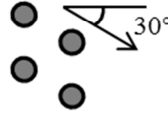
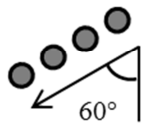
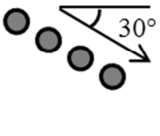
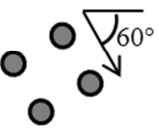
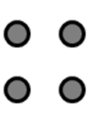
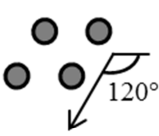
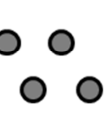


**Figure 7.** Annual energy production (AEO) as a function of WEC distance for square arrays with different orientations: (a) Alghero, (b) Mazara del Vallo, (c) Ponza and (d) La Spezia. Black lines represent AEO of four isolated WECs.





**Figure 8.** Annual energy production (AEO) as a function of WEC distance for rhombus arrays with different orientations: (a) Alghero, (b) Mazara del Vallo, (c) Ponza and (d) La Spezia. Black lines represent AEO of four isolated WECs.

Alghero	-5.8%	+1.3%
		
	d = 5D	d = 10D
	-3.2%	+1%
		
	d = 5D	d = 20D
	-5.1%	+1.5%
		
	d = 5D	d = 20D
Mazara	-5.5%	+3.4%
		
	d = 5D	d = 5D
	-2.1%	+1.3%
		
	d = 5D	d = 20D
	-3.9%	+1.7%
		
	d = 5D	d = 20D
Ponza	-5.7%	+3.2%
		
	d = 5D	d = 5D
	-1.5%	+1.5%
		
	d = 5D	d = 20D
	-3.6%	+2.1%
		
	d = 5D	d = 10D
La Spezia	-5.1%	+3.3%
		
	d = 5D	d = 5D
	-2.1%	+1.3%
		
	d = 5D	d = 20D
	-3.8%	+1.6%
		
	d = 5D	d = 20D

**Figure 9.** Wave farm designs maximizing/minimizing the annual energy production at the study sites and associated energy gain (green) and loss (red). North pointing towards the top of the page.

Wave farms are simulated in the time domain by a hydrodynamic-electromagnetic model

The effects of design parameters on array performance are investigated

A site-specific design optimization is carried out for different Italian wave climates

Wave interactions are negligible if WECs are separated by at least 10 buoy diameters

Arrays should be oriented to maximize the power production for the dominant wave direction